



On the Boussinesq approximation in arbitrarily accelerating frames of reference

Hugh M. Blackburn^{1,†}, Juan M. Lopez², Jagmohan Singh¹ and Alexander J. Smits³

¹Department of Mechanical and Aerospace Engineering, Monash University, Clayton, VIC 3800, Australia

²School of Mathematics and Statistical Sciences, Arizona State University, Tempe, AZ 85287, USA

³Department of Mechanical and Aerospace Engineering, Princeton University, Princeton, NJ 08544, USA

(Received 5 May 2021; revised 23 June 2021; accepted 12 July 2021)

This work examines consequences of modelling approximation errors made within the context of the Navier–Stokes–Boussinesq system. Starting from a canonical Boussinesq model, where density fluctuations are allowed to interact with all accelerative terms of the incompressible Navier–Stokes equations in arbitrarily accelerating reference frames, a unified treatment is developed that provides a straightforward way to identify buoyancy forcing associated with gravitational effects, centrifugal forcing associated with frame rotation, as well as centrifugal-type forcing due to variations in flow kinetic energy. The results of the cases studied in inertial, rotating and mixed reference frames demonstrate that in general it may be important to apply buoyancy effects to all non-local accelerative terms, including non-gradient terms such as Coriolis acceleration. Additionally, it is shown that the common practice of ignoring terms representing interaction between density fluctuation and local fluid acceleration can lead to non-negligible error in Boussinesq modelling of highly unsteady flows. These findings have special significance for accurate simulation of flows with density variations in which there may be both background rotation and localised regions of strong swirl, but are also relevant for studies conducted in the inertial frame of reference.

Key words: buoyancy-driven instability, rotating flows, general fluid mechanics

1. Introduction

The Boussinesq approximation for flows with buoyancy – that if density variations are small enough then the flow can be considered incompressible, and that buoyancy body-force contributions arise in the momentum equations – has been widely used for many years. The conditions under which the approximation is adequate if the underlying

† Email address for correspondence: hugh.blackburn@monash.edu

driving force for buoyancy is gravity have been discussed in detail by Tritton (1988). Since the effects of uniform gravitational acceleration can be replaced by a suitable rectilinear acceleration of the reference frame in which the flow is considered, buoyant flows driven by gravity can be considered as the simplest case of flows with density variation arising in arbitrarily accelerating frames. The most general case allows for frame rotation in addition to rectilinear acceleration of the origin, and this is what we seek to address herein.

When the reference frame rotates, centrifugal buoyancy can be considered in addition to gravitational: heavier fluid moves outwards from the axis of rotation owing to centrifugal force, and *vice versa* (see e.g. Barcilon & Pedlosky 1967; Brummell, Hart & Lopez 2000; Hart 2000; Marques *et al.* 2007). However, these centrifugal buoyancy effects must also exist in flows with localised swirl, irrespective of the frame of reference. Such effects were considered by Lopez, Marques & Avila (2013), who suggested that, in a non-rotating frame, centrifugal buoyancy forcing could be approximated as arising from the product of density fluctuation and the gradient of kinetic energy. How one should model centrifugal buoyancy when both the reference frame rotates and there is also significant localised swirl has been left unaddressed. Such considerations may be important, for example, in simulations of rotating machinery flows. For these flows, it is convenient to work in a rotating frame where the geometry appears stationary, but where localised swirl and associated centrifugal buoyancy effects are comparable to those associated with frame rotation. More generally, these considerations can become important when there is no obvious choice for an appropriate frame rotation rate, such as when there are differentially rotating parts of the geometry.

In the following, we consider the question of how best to model the effects of Boussinesq buoyancy in cases of general frame motion while also including centrifugal buoyancy due to localised swirl. The approach taken builds on, and generalises, the work by Lopez *et al.* (2013) in that density (and its variation) is allowed to interact with all non-local fluid acceleration terms. An approach introduced earlier by Marques *et al.* (2007) and reconsidered by Lopez *et al.* (2013) – that density fluctuations are considered to be significant in the momentum equations only where they premultiply terms representing the gradient of a scalar – is examined, generalised and shown to be adequate in some situations but not others. We also show that the general practice of ignoring the effect of interaction between density variations and local fluid acceleration, common in Boussinesq approximations, can produce significant errors, increasing as the local accelerative terms become larger in relation to advective and frame-accelerative terms. Those errors should, if possible, be minimised by an appropriate choice of reference frame. Our results are necessarily obtained by computer simulation since analytical solutions are not available; however, we have used sufficient numerical resolution to ensure that errors incurred by approximate modelling rather than numerical approximation errors remain the central focus. The differences in computational resources required to solve the various forms of models considered are minimal.

2. Formulation

The Boussinesq approach to modelling buoyant flows can be summarised by stating that comparatively minor changes in density are accommodated within the incompressible Navier–Stokes system without changes to fluid properties, such as viscosity and diffusivity. The Boussinesq model is an approximation to the more complete, but computationally expensive, compressible Navier–Stokes system. A standard requirement for good Boussinesq approximations is that the density fluctuations relative to a

background density be small, $\rho'/\rho_0 \ll 1$ (e.g. see Tritton 1988). With this in mind, the momentum and continuity equations for a Newtonian fluid can be written as

$$\frac{\rho}{\rho_0} \frac{D\mathbf{u}}{Dt} = \left(1 + \frac{\rho'}{\rho_0}\right) \frac{D\mathbf{u}}{Dt} = -\frac{1}{\rho_0} \nabla p + \nu \nabla^2 \mathbf{u}, \quad \nabla \cdot \mathbf{u} = 0, \quad (2.1a,b)$$

where $D\mathbf{u}/Dt$ is the material derivative of velocity, ρ_0 is a constant reference density, ρ' is the density fluctuation and p is the pressure. The kinematic viscosity ν is a constant determined at a temperature corresponding to ρ_0 . The set (2.1a,b) might be termed the canonical form of the Navier–Stokes–Boussinesq system. A sometimes overlooked fact of Boussinesq-based modelling is that the maximum relative density variation, ρ'_{\max}/ρ_0 , is an independent dimensionless variable and should be sufficiently small for the approximation to be valid.

For general reference frame motion, the material derivative is

$$\frac{D\mathbf{u}}{Dt} = \frac{\partial \mathbf{u}}{\partial t} + \mathbf{u} \cdot \nabla \mathbf{u} + 2\boldsymbol{\Omega} \times \mathbf{u} + \boldsymbol{\Omega} \times (\boldsymbol{\Omega} \times \mathbf{r}) + \boldsymbol{\alpha} \times \mathbf{r} + \mathbf{A}, \quad (2.2)$$

where $\partial \mathbf{u}/\partial t$ is the local rate of change of velocity, $\mathbf{u} \cdot \nabla \mathbf{u}$ is its convective rate of change, \mathbf{A} is a rectilinear acceleration of the frame origin, $\boldsymbol{\Omega}$ is frame angular velocity around the origin, $\boldsymbol{\alpha} = d\boldsymbol{\Omega}/dt$ is the angular acceleration of the frame around the origin and \mathbf{r} is a position vector relative to the origin. The velocity is measured relative to the frame's origin. The terms $2\boldsymbol{\Omega} \times \mathbf{u}$, $\boldsymbol{\Omega} \times (\boldsymbol{\Omega} \times \mathbf{r})$ and $\boldsymbol{\alpha} \times \mathbf{r}$ are respectively known as Coriolis, centripetal and Euler accelerations. Since acceleration of the origin is a uniform vector field, it can be written as the gradient of a scalar field Φ that varies linearly with position, i.e. $\mathbf{A} = \nabla(\mathbf{A} \cdot \mathbf{r}) = \nabla\Phi$. Using standard vector identities, the material derivative may be rewritten as

$$\begin{aligned} \frac{D\mathbf{u}}{Dt} &= \frac{\partial \mathbf{u}}{\partial t} + \boldsymbol{\omega} \times \mathbf{u} + \nabla\left(\frac{1}{2}|\mathbf{u}|^2\right) + 2\boldsymbol{\Omega} \times \mathbf{u} + \nabla\left(\frac{1}{2}|\boldsymbol{\Omega} \times \mathbf{r}|^2\right) + \boldsymbol{\alpha} \times \mathbf{r} + \nabla\Phi \\ &= \frac{\partial \mathbf{u}}{\partial t} + \boldsymbol{\omega} \times \mathbf{u} + 2\boldsymbol{\Omega} \times \mathbf{u} + \boldsymbol{\alpha} \times \mathbf{r} + \nabla\left(\frac{1}{2}|\mathbf{u}|^2 + \frac{1}{2}|\boldsymbol{\Omega} \times \mathbf{r}|^2 + \Phi\right), \end{aligned} \quad (2.3)$$

in which $\boldsymbol{\omega} = \nabla \times \mathbf{u}$ is the vorticity. Without loss of generality, a uniform gravitational force per unit mass, \mathbf{g} , may be replaced by an equivalent frame acceleration $\mathbf{A} = -\mathbf{g}$, implying also a change in sign of the scalar field Φ . The gradient term representing centripetal acceleration is often written as $-|\boldsymbol{\Omega}|^2 \mathbf{r}_\perp$, where \mathbf{r}_\perp is the radius vector taken perpendicular to the axis of rotation.

A further approximation often applied in concert with that of Boussinesq is to include the effect of density fluctuation only on non-local acceleration terms. This allows density fluctuation effects to be dealt with explicitly in time (as is typically done for the nonlinear terms in uniform-density flows, which is convenient for many time-stepping numerical schemes). Within the context of the canonical Boussinesq approach, this is completely correct for steady flows and approximately so if the local acceleration terms are small compared to the sum of the others. Applying this idea to (2.2), equation (2.3) gives

$$\begin{aligned} \frac{\rho}{\rho_0} \frac{D\mathbf{u}}{Dt} &\approx \frac{\partial \mathbf{u}}{\partial t} + \left(1 + \frac{\rho'}{\rho_0}\right) [\mathbf{u} \cdot \nabla \mathbf{u} + 2\boldsymbol{\Omega} \times \mathbf{u} + \boldsymbol{\Omega} \times (\boldsymbol{\Omega} \times \mathbf{r}) + \boldsymbol{\alpha} \times \mathbf{r} + \mathbf{A}] \\ &= \frac{\partial \mathbf{u}}{\partial t} + \left(1 + \frac{\rho'}{\rho_0}\right) [\boldsymbol{\omega} \times \mathbf{u} + 2\boldsymbol{\Omega} \times \mathbf{u} + \boldsymbol{\alpha} \times \mathbf{r} + \nabla\left(\frac{1}{2}|\mathbf{u}|^2 + \frac{1}{2}|\boldsymbol{\Omega} \times \mathbf{r}|^2 + \Phi\right)]. \end{aligned} \quad (2.4)$$

Since the final group of terms is the gradient of a scalar, (2.4) can be further rearranged in order to remove consideration of hydrostatic-type variations in pressure, to give

$$\frac{\partial \mathbf{u}}{\partial t} + \left(1 + \frac{\rho'}{\rho_0}\right) [\boldsymbol{\omega} \times \mathbf{u} + 2\boldsymbol{\Omega} \times \mathbf{u} + \boldsymbol{\alpha} \times \mathbf{r}] + \frac{\rho'}{\rho_0} \nabla \left(\frac{1}{2}|\mathbf{u}|^2 + \frac{1}{2}|\boldsymbol{\Omega} \times \mathbf{r}|^2 + \Phi\right). \quad (2.5)$$

All forms of (2.4) and (2.5) represent the same rational generalisation of the treatment given by (2.12) of Lopez *et al.* (2013) in order to deal with arbitrarily accelerating frames of reference. When using this approach in simulations, special treatment or separation of the scalar-gradient-type terms is not required; we have written them as separate terms here partly to aid the exposition below. We point out that Lopez *et al.* (2013) essentially gave two alternative treatments: one – their (2.4) – for rotating frames of reference with gravity, and the other – their (2.12) – for inertial frames of reference with gravity. The present unified approach can deal with either frame as a special case and it can help explain why using (2.4) and (2.12) of Lopez *et al.* (2013) will in general give different outcomes if applied to the same flow.

The gradient-type buoyancy-related terms in (2.5) result from: (i) centrifugal buoyancy related to (perhaps localised) swirl with respect to the reference frame, $\nabla(|\mathbf{u}|^2/2)$; (ii) centrifugal buoyancy due to uniform frame rotation (sometimes referred to as ‘Coriolis buoyancy’), $\nabla(|\boldsymbol{\Omega} \times \mathbf{r}|^2/2)$; and (iii) buoyancy due to gravity/frame acceleration, $\nabla\Phi$. The term $\nabla(|\mathbf{u}|^2/2)$ is clearly the gradient of kinetic energy per unit mass considered in the frame of reference, and its buoyancy effect does not appear to have an accepted name. However, for flows that are solid-body rotation, considered in an inertial reference frame (such that $\boldsymbol{\Omega} = 0$), it is straightforward to show that it is also associated with centrifugal effects. Note that $\rho'\nabla(|\mathbf{u}|^2/2)$ appears as a forcing term in (2.14) of Lopez *et al.* (2013), who derived it on the basis of an approximation; when considered as an accelerative term rather than a forcing term, it takes the opposite sign to our outcome.

Up to this point we have not discussed how density variations are computed. We use a standard treatment where the relative density variations arise via a constant temperature-dependent volumetric expansion rate β , such that

$$\rho'/\rho_0 = \beta(T_{\text{ref}} - T) = (T_{\text{ref}} - T)/T_{\text{ref}}, \quad (2.6)$$

where T is absolute temperature, T_{ref} is a reference or background value and the latter relation is appropriate to a perfect gas. Very often, $T_{\text{ref}} = (T_{\text{hot}} + T_{\text{cold}})/2$, in which case $\rho'_{\text{max}}/\rho_0 = (T_{\text{hot}} - T_{\text{cold}})/(T_{\text{hot}} + T_{\text{cold}}) = \Delta T/(2T_{\text{ref}}) = \beta\Delta T/2$. To compute transport of temperature, we use an advection–diffusion equation

$$\frac{\partial T}{\partial t} + \mathbf{u} \cdot \nabla T = \kappa \nabla^2 T, \quad (2.7)$$

where $\kappa = \nu/Pr$ is the fluid’s thermal diffusivity and Pr is the Prandtl number. Equation (2.7) represents the first law of thermodynamics under standard Boussinesq restrictions (see e.g. Tritton 1988). More generally, e.g. for thermohaline buoyancy, more complicated approaches could be used to estimate ρ'/ρ_0 ; provided this remains small, there are no consequences for the key findings of § 3.

In all computations reported in § 3, we have employed a public-domain spectral element code for incompressible flows (Blackburn *et al.* 2019) and checked that outcomes are effectively resolution-independent. In summary, we solve the (approximate) unsteady

incompressible Navier–Stokes–Boussinesq equations

$$\begin{aligned} \frac{\partial \mathbf{u}}{\partial t} + \left(1 + \frac{\rho'}{\rho_0}\right) [\boldsymbol{\omega} \times \mathbf{u} + 2\boldsymbol{\Omega} \times \mathbf{u} + \boldsymbol{\alpha} \times \mathbf{r}] + \frac{\rho'}{\rho_0} \nabla \left(\frac{1}{2}|\mathbf{u}|^2 + \frac{1}{2}|\boldsymbol{\Omega} \times \mathbf{r}|^2 + \Phi\right) \\ = -\nabla \check{p} + \nu \nabla^2 \mathbf{u}, \quad \nabla \cdot \mathbf{u} = 0, \end{aligned} \quad (2.8a,b)$$

where \check{p} may include hydrostatic variations to the normalised pressure p/ρ_0 , together with the advection–diffusion equation (2.7), coupled via (2.6). The non-local accelerative terms of (2.8a,b) can be selectively enabled to examine their effects.

In both Marques *et al.* (2007) and Lopez *et al.* (2013), it was argued, on the basis that neglected terms should be of second order, that only gradient density-fluctuation effects need be retained in order to obtain first-order-accurate results with Boussinesq-type buoyancy. In what follows we will demonstrate that this may lead to significant error in some cases, even for small density fluctuations. One can choose to include all the buoyancy-related terms in (2.8a,b), or to include only those which factor gradients of a scalar function (effectively, the proposal of Marques *et al.* (2007), but here generalised to arbitrarily accelerating frames). The difference between these two approaches should only amount to the inclusion or omission of terms in the momentum equations such as

$$\frac{\rho'}{\rho_0} [\boldsymbol{\omega} \times \mathbf{u} + 2\boldsymbol{\Omega} \times \mathbf{u} + \boldsymbol{\alpha} \times \mathbf{r}] = \frac{\rho'}{\rho_0} [(\boldsymbol{\omega} + 2\boldsymbol{\Omega}) \times \mathbf{u} + \boldsymbol{\alpha} \times \mathbf{r}], \quad (2.9)$$

where $\boldsymbol{\omega} + 2\boldsymbol{\Omega}$ is twice the local fluid rotation rate in the inertial frame. We shall demonstrate that omission of terms (2.9) can have a significant effect on the accuracy of outcomes, though we restrict attention to cases where $\boldsymbol{\alpha} = 0$.

3. Numerical results

Our approach is to investigate two simple case studies that possess both rotation and buoyancy, and can be considered in various reference frames, such as in an inertial frame with walls moving relative to the observer, in a rotating frame in which the walls appear fixed, and in an intermediate ‘semi-rotating’ frame. For both case studies, no flow other than solid-body rotation would arise in the absence of centrifugal buoyancy effects. The first test case is an axisymmetric restriction of the flow considered by Marques *et al.* (2007), while the second is an axially invariant version of the flow configuration considered by Pitz, Marxen & Chew (2017). Both cases have non-slip walls, so that far-field boundary conditions (and how these might need to account for hydrostatic pressure gradients) do not require detailed examination, and both have $\boldsymbol{\alpha} = 0$.

3.1. Axisymmetric steady flow

The first case is the same as that examined in § 3.1 of Marques *et al.* (2007); axisymmetric flow in a rotating cylindrical container of radius-to-length aspect ratio $R/L = 1$, heated on one endwall and cooled on the other, with an adiabatic outer wall. In their treatment, gravitational acceleration acts in the direction pointing from the cool wall to the hot wall, and the Prandtl number $Pr = 7$, i.e. the modelled flow is that of water in a rotating cylinder heated from below. They used $(\rho'/\rho_0)\nabla(|\boldsymbol{\Omega} \times \mathbf{r}|^2/2 + \Phi)$ for the buoyancy terms, $\rho'_{\max}/\rho_0 = 0.031429$, and omitted the gradient of kinetic energy as well as the terms in (2.9). In the absence of centrifugal buoyancy, the basic state consists of uniform conduction and solid-body rotation. For non-zero Froude number, $Fr = |\boldsymbol{\Omega}|^2 R/|g|$, the saturated states (prior to onset of any instability) are steady toroidal overturning motion

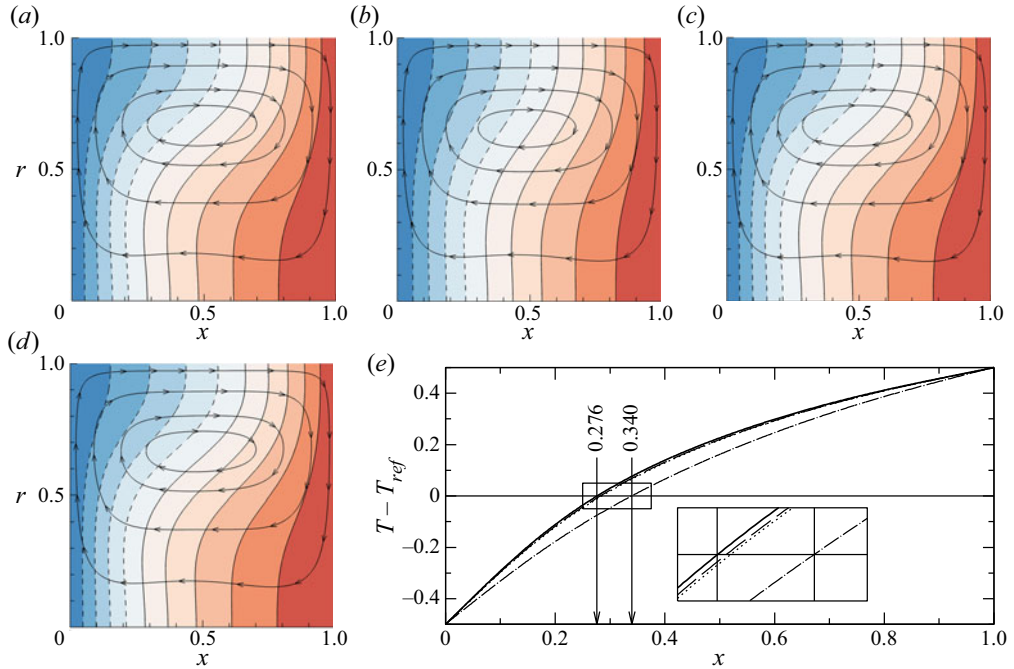


Figure 1. Simulation results for the axisymmetric test case of § 3.1 of Marques *et al.* (2007). Panels (a–d) illustrate flows in the meridional (x, r) semiplane; the cylinder rotates around the x axis. The gravity vector is aligned with the $+x$ axis, or, equivalently, frame acceleration is aligned with $-x$. Colour contours are of $T - T_{ref}$ drawn at levels -0.5 to $+0.5$ in steps of 0.1 , and dashed lines represent negative values. Sectional streamlines illustrate meridional flows. (a–c) Flows computed using gradient-type buoyancy, respectively in inertial, semi-rotating and fully rotating frames of reference. (d) The same quantities computed using the more complete approach of (2.8a,b) – the same in all frames of reference. (e) Temperature profiles extracted along the axis (inset shows detail around the zero crossings). The solid line shows data from the results of (d); the dotted, chained and dashed lines show data from (a), (b) and (c), respectively; the semi-rotating case (b) differs significantly from the others.

with upwelling of warm fluid along the axis and a return flow of cooled fluid near the outer wall. The remaining dimensionless groups (of total six) are: maximum relative density variation ρ'_{max}/ρ_0 ; Rayleigh number $Ra = \beta|g|L^3(T_{hot} - T_{cold})/\kappa\nu$; and Coriolis number $Co = |\Omega|L^2/\nu$.

Figure 1 presents results from our axisymmetric simulation at $Fr = 0.4$, $Co = 100$ and $Ra = 1.1 \times 10^{-4}$; the same parameter values as used for the simulation in figure 1 of Marques *et al.* (2007). The resulting flows are steady, $\partial \mathbf{u}/\partial t = 0$, in all frames of reference. We take $T_{hot} - T_{cold} = 1$, and so in (2.6) $T_{ref} \equiv 15.909$. The flow visualisations shown in figure 1(a–d) are presented in the meridional (x, r) semiplane and rotation is around the x axis; lengths are normalised by the cylinder radius R .

Figure 1(a–c) represent computations made using the gradient-based buoyancy approach, i.e. where the terms of (2.9) are omitted, respectively for the inertial frame of reference (where walls rotate at the vessel rotation rate $|\Omega|$), the semi-rotating frame (walls rotate at rate $|\Omega|/2$) and the fully rotating frame of reference (in which the walls appear fixed). One may observe that the results in panels (a) and (c) are much alike, and very similar to those in figure 1 of Marques *et al.* (2007), while those in panel (b), while superficially similar, differ significantly in detail from panels (a) and (c); note,

for example, the locations of the $T = 0$ contours (the first solid lines) along the rotation axis, x .

Figure 1(d) shows results using the more complete approach where the terms of (2.9) are retained in (2.8a,b). In this case, meridional flows and temperature contours for all three frames of reference are identical to within numerical error (here, at relative levels approximately nine orders of magnitude or more below the outcomes presented). This agreement demonstrates the completeness of the approach advocated in (2.8a,b) for steady flows.

Figure 1(e) shows profiles of temperature extracted along the rotation axis for the various approaches of figure 1(a–d). From these, the locations for $T = 0$ on the x axis can be read more precisely. Again, we note the relatively good agreement of panels (a) and (c), and that these agree well with those of panel (d), while results obtained with the gradient-only buoyancy approach in the semi-rotating frame, panel (b), are significantly in error.

3.2. Non-axisymmetric flow

Our second case study is a simple adaptation of the rotating annular cavity flow considered by Pitz *et al.* (2017), with a hot outer wall and cold inner wall. This case considers a zero-gravity environment, and so centrifugal buoyancy is wholly responsible for driving azimuthal flow variations. We focus on the geometry with inner-to-outer radius ratio $\eta = a/b = 0.52$, as was the case in most of their work. To simplify matters, we compute two-dimensional flows that are axially invariant, while most of their results were for a fully enclosed cavity with adiabatic endwalls. In the absence of gravity and endwalls, the five independent dimensionless groups may be represented as η , Pr , ρ'_{max}/ρ_0 , $Re = |\boldsymbol{\Omega}|(b+a)(b-a)/2\nu$ and $Ra = \beta(T_{hot} - T_{cold})|\boldsymbol{\Omega}|^2(b+a)(b-a)^3/2\kappa\nu$. As in Pitz *et al.* (2017), we use $Pr = 0.7$ (air) and $\rho'_{max}/\rho_0 = 0.05$. Pitz *et al.* (2017) carried out computations in a rotating frame of reference, included only the gradient-based centripetal acceleration term $(\rho'/\rho_0)\nabla(|\boldsymbol{\Omega} \times \mathbf{r}|^2/2)$ in their approximation to (2.8a,b), and, like Marques *et al.* (2007), omitted the terms of (2.9). Pitz *et al.* found that the fully enclosed flow bifurcated to a (standing) wave, steady in the rotating frame, with azimuthal wavenumber $k = 5$ at $Ra = 3040$ (see their table 1).

This case is somewhat more complicated than the one considered in § 3.1, largely because of the possibility of unsteady flow at the onset of instability. This enables us to additionally examine the consequences of committing the (standard) modelling approximation error of omitting term $(\rho'/\rho_0)\partial\mathbf{u}/\partial t$ from (2.1a,b). We mainly focus on the critical Rayleigh numbers, which are typically substantially smaller than those of Pitz *et al.* (2017). This difference is due to the effects of endwalls, which were present for their study, but are absent in ours. We first compute the stable one-dimensional rotating basic state at $Ra = 1500$, add a small white-noise perturbation everywhere in the domain at higher Rayleigh numbers, wait for saturated two-dimensional states to evolve, then reduce the Rayleigh number and repeat until the bifurcation is suitably bracketed. This is detected by subtracting the stable basic state and computing the domain integral of kinetic energy in the difference flow; since the bifurcation is of supercritical Hopf type, this energy integral initially varies linearly with the control parameter, Rayleigh number, at onset (Guckenheimer & Holmes 1986). As in the case study of § 3.1, we have carried out simulations in inertial, rotating and semi-rotating frames of reference using both the near-complete approach of (2.8a,b), and the gradient-only approach in which the terms (2.9) are omitted. In all cases, instability is a supercritical Hopf bifurcation to azimuthal waves with $k = 5$. Figure 2 shows a snapshot of temperature contours obtained using the

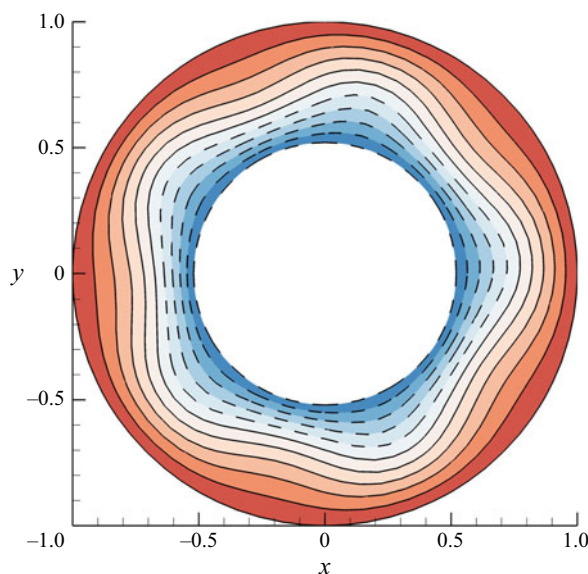


Figure 2. Simulation results for a two-dimensional flow in a rotating annulus at $Ra = 1850$, with centrifugal buoyancy. This is an axially invariant equivalent of the annulus of radius ratio $\eta = 0.52$ considered by Pitz *et al.* (2017). Colour contours of $T - T_{ref}$ range from -1 at the inner radius (blue) to $+1$ at the outer radius (red), in steps of 0.2 ; dashed lines represent negative values.

computational technique represented by (2.8a,b), obtained in the fully rotating frame at $Ra = 1850$, illustrating the $k = 5$ wave.

In table 1, critical Rayleigh numbers Ra_c for our two-dimensional simulations are presented, along with their percentage variations from the ‘true’ value obtained using the approach of (2.8a,b). (We have refined spatial meshes and time step sizes to the point that relative numerical errors of the values presented are well below the accuracy suggested by the number of significant figures provided.) The solution obtained in the fully rotating frame for the ‘non-gradient’ equation set (2.8a,b) is a slow retrograde rotating wave; its rotation speed relative to the reference frame is -2.515×10^{-3} . We have also carried out a bifurcation study for a frame in which this wave appears fixed, thus making the local accelerations $\partial \mathbf{u} / \partial t = 0$. This is the ‘true’ reference case from which the errors in Ra_c shown in table 1 were calculated. To approximately five significant figures, $Ra_c = 1759$ for this case agrees with that obtained for the fully rotating frame of reference when the ‘complete’ approach of (2.8a,b) is employed. In this two-dimensional restriction, Ra_c is well below that in the full three-dimensional study of Pitz *et al.* (2017), and somewhat above the value for Rayleigh–Bénard convection rolls between two parallel planes, $Ra = 1708$ (Chandrasekhar 1961).

Considering the differences in estimates of Ra_c in table 1, we first note that for the inertial and semi-rotating frames, all solutions are rotating waves, and in the inertial frame ($\Omega = 0$), the waves rotate at very close to the rotation rate of the annulus. In the fully rotating frame ($\Omega = 1$) and for the non-gradient approach, the solution is a very slow rotating wave. We have already seen that for the steady flows, as considered in § 3.1, the non-gradient and the more complete Boussinesq approximations produce identical results (modulo solid-body rotation) in all frames. Thus we can attribute the increasing error in Ra_c as Ω decreases for the non-gradient results listed in table 1 to the fact that $(\rho' / \rho_0) \partial \mathbf{u} / \partial t$, a term neglected in all our and, as far as we are aware, all extant Boussinesq

Ω	Non-gradient		Gradient	
0	1824	(3.7 %)	1735	(−1.3 %)
0.5	1777	(1.0 %)	3489	(98.4 %)
1	1759	(0.0 %)	1754	(−0.3 %)

Table 1. Critical Rayleigh numbers, Ra_c , with relative errors, for the non-axisymmetric case study shown in figure 2. Ω is the dimensionless rotation rate of the frame of reference used, varying between zero (inertial) and unity (fully rotating). A reference case, with $\Omega = 0.997485$ was used to compute the error values listed (see text).

approximations, becomes more important when the flow becomes increasingly unsteady as Ω decreases below 0.997485 towards zero. Provided $\rho'/\rho_0 \ll 1$, such errors should always be relatively small. For the present calculations, the maximum error in Ra_c for the non-gradient approach, 3.7 %, is of the same order as ρ'_{max}/ρ_0 , 5 %.

Table 1 also shows that, for the gradient-based Boussinesq approximation, errors in Ra_c are relatively small when $\Omega = 0$ and 1, but very large for the semi-rotating case with $\Omega = 0.5$. This is mainly attributable to omitting the terms represented in (2.9), which are apparently significant for the semi-rotating case. Recall that for the steady flow of § 3.1, the error for the gradient-based approach was also largest in the semi-rotating case. Finally, for $\Omega = 1$ there is a distinction in bifurcation behaviour between the two Boussinesq approaches. While for the non-gradient approach, the bifurcation is to a rotating wave, for the gradient approach, a standing wave bifurcates. Theoretically, if the modelled physics were equivalent, these two wave types would bifurcate linearly at the same value of Ra_c , and (weakly) nonlinear effects would select one of these two outcomes as the stable case, observable using nonlinear simulations. Therefore, changing the modelled physics (from non-gradient- to gradient-based buoyancy) here also changes the nature of the bifurcation.

4. Discussion and conclusions

The main points of novelty in the present work are as follows:

- (i) We have supplied a frame-independent exposition of Boussinesq modelling which could be used for accurate simulation of flows with differential rotation where there is no distinguished frame of reference; such conditions could, for example, be obtained in rotating machinery of various kinds.
- (ii) We have demonstrated that a modelling restriction to include only gradient-type buoyancy terms, as advocated for example by Marques *et al.* (2007) and Lopez *et al.* (2013), can lead to errors which are sometimes of first-order significance. In § 3.1 we have shown that when dealing with a steady flow, our unified approach eliminates these modelling errors in a frame-independent way.
- (iii) We have shown that in very unsteady flows, omission of terms of type $(\rho'/\rho_0)\partial\mathbf{u}/\partial t$ from (2.1a,b) can lead to non-negligible modelling errors. We were able to do this by considering in § 3.2 a flow which could be made steady by a suitable choice of rotating frame, and examining the size of errors in Ra_c for various other frames where $|\partial\mathbf{u}/\partial t|$ becomes large.

All Boussinesq approaches represent approximations to the fully compressible Navier–Stokes system of equations. One might consider (2.1a,b), in which density factors all terms of the material derivative of velocity, to represent the canonical form of the

Boussinesq approximation. As far as we are aware, however, it is standard (and convenient) practice to omit the effect of density variation on the local derivative, i.e. terms of form $(\rho'/\rho_0)\partial\mathbf{u}/\partial t$, which in the canonical case leads to (2.8a,b). In § 3.1, it was demonstrated that for a steady flow, that approach produces the same result in all steadily accelerating frames of reference. In § 3.2, however, it was shown that such an approach may introduce significant error, perhaps of order ρ'_{\max}/ρ_0 , if $\partial\mathbf{u}/\partial t$ is large compared to non-local accelerations. An obvious and standard way to minimise errors of this kind is to adopt an appropriate frame of reference in which local acceleration terms are as small as possible. If the flow is dominated by a known background rotation, this is the frame to use. A difficulty arises if the appropriate rate is unclear in advance, e.g. where there is significant differential rotation and unsteady flow.

When one is assured that background rotation provides the dominant centrifugal buoyancy effect, it appears reasonable to deal with this using only gradient-based buoyancy. In an inertial frame where $\boldsymbol{\Omega} = 0$, this may be addressed via $(\rho'/\rho_0)\nabla(|\mathbf{u}|^2/2)$. Alternatively, in a fully rotating frame one may reasonably use $(\rho'/\rho_0)\nabla(|\boldsymbol{\Omega} \times \mathbf{r}|^2/2) = -(\rho'/\rho_0)|\boldsymbol{\Omega}|^2\mathbf{r}_\perp$: for solid-body rotation (i.e. which flows with dominant background rotation approximate to first order) the two forms are equivalent. The difficulty again arises when there is no clear choice of frame, e.g. when there is significant differential rotation. In that case, approaches which employ only gradient-type buoyancy terms may lead to significant errors, as the results of § 3 make clear.

Initially, it seems confusing that the results obtained when the terms (2.9) are omitted are frame-dependent, since the form of these terms is frame-invariant. However, the term $\boldsymbol{\omega} \times \mathbf{u}$ arises from the identity $\mathbf{u} \cdot \nabla \mathbf{u} = \boldsymbol{\omega} \times \mathbf{u} + \nabla(|\mathbf{u}|^2/2)$. The partition between the non-gradient and gradient components of this decomposition varies depending on the reference frame adopted, and hence so does the relative importance of the product term $(\rho'/\rho_0)\boldsymbol{\omega} \times \mathbf{u}$ neglected in the gradient-based approach. Clearly, this term can become significant in ‘semi-rotating’ frames. We conclude that it is always safest to retain such terms and use one of the forms (2.4) or (2.5), leading to (2.8a,b).

The formulation of (2.8a,b) is simply a straightforward generalisation of the methodology advanced in § 2.2.2 of Lopez *et al.* (2013) for use in an inertial frame of reference, so as to accommodate arbitrary frame acceleration. However, in their further development (§ 2.2.3), Lopez *et al.* sought to derive a gradient-type centrifugal effect based on an approximation for rapidly rotating frames (their (2.13)). That approximation is incorrect, since it results in a forcing term $\rho'\nabla(|\mathbf{u}|^2/2)$ for the Navier–Stokes equations. Transposed so as to be interpreted as an accelerative term, as we have considered in (2.8a,b), this would become $-\rho'\nabla(|\mathbf{u}|^2/2)$, taking the opposite sign to our derivation.

Funding. This research was supported by Australian Research Council Discovery Project grant DP160103961 and U.S. National Science Foundation grant 1929139.

Declaration of interests. The authors report no conflict of interest.

Author ORCIDs.

 Hugh M. Blackburn <https://orcid.org/0000-0003-3469-5237>;

 Juan M. Lopez <https://orcid.org/0000-0002-4580-6505>;

 Jagmohan Singh <https://orcid.org/0000-0002-4688-0643>;

 Alexander J. Smits <https://orcid.org/0000-0002-3883-8648>.

REFERENCES

- BARCILON, V. & PEDLOSKY, J. 1967 On the steady motions produced by a stable stratification in a rapidly rotating fluid. *J. Fluid Mech.* **29**, 673–690.

Boussinesq approximation in accelerating frames

- BLACKBURN, H.M., LEE, D., ALBRECHT, T. & SINGH, J. 2019 Semtex: a spectral element–Fourier solver for the incompressible Navier–Stokes equations in cylindrical or Cartesian coordinates. *Comput. Phys. Commun.* **245**, 106804.
- BRUMMELL, N., HART, J.E. & LOPEZ, J.M. 2000 On the flow induced by centrifugal buoyancy in a differentially-heated rotating cylinder. *Theor. Comput. Fluid Dyn.* **14**, 39–54.
- CHANDRASEKHAR, S. 1961 *Hydrodynamic and Hydromagnetic Stability*. Oxford University Press. Dover edn, 1981.
- GUCKENHEIMER, J. & HOLMES, P. 1986 *Nonlinear Oscillations, Dynamical Systems, and Bifurcations of Vector Fields*. Applied Mathematical Sciences, vol. 42. Springer, 2nd print.
- HART, J.E. 2000 On the influence of centrifugal buoyancy on rotating convection. *J. Fluid Mech.* **403**, 133–151.
- LOPEZ, J.M., MARQUES, F. & AVILA, M. 2013 The Boussinesq approximation in rapidly-rotating flows. *J. Fluid Mech.* **737**, 56–77.
- MARQUES, F., MERCADER, I., BATISTE, O. & LOPEZ, J.M. 2007 Centrifugal effects in rotating convection: axisymmetric states and three-dimensional instabilities. *J. Fluid Mech.* **580**, 303–318.
- PITZ, D.B., MARXEN, O. & CHEW, J.W. 2017 Onset of convection induced by centrifugal buoyancy in a rotating cavity. *J. Fluid Mech.* **826**, 484–502.
- TRITTON, D.J. 1988 *Physical Fluid Dynamics*, 2nd edn. Oxford University Press.